SCIRES it
SCIentific RESearch and Information Technology
Ricerca Scientifica e Tecnologie dell'Informazione
Vol 15, Issue 2 (2025), 215-232
e-ISSN 2239-4303, DOI 10.2423/i22394303v15n2p215

CASPUR-CIBER Publishing, http://www.sciresit.it

BEHAVIORAL ASSESSMENT AND OPTIMIZATION OF PEDESTRIAN FLOOD EVACUATION IN HISTORIC URBAN SETTINGS: A MULTISCALE SIMULATION APPROACH TO RISK MITIGATION

Guido Romano, Gabriele Bernardini*, Fabrizio Marinelli**, Andrea Pizzuti**, Marco D'Orazio*, Enrico Quagliarini**

* DICEA Department, Università Politecnica delle Marche, Ancona, Italy
** DII Department, Università Politecnica delle Marche, Ancona, Italy

Abstract

Digital technologies can significantly support flood risk assessment and mitigation in Historic Urban Built Environments (HUBEs). Simulation tools can manage such complex disaster scenarios and provide useful analysis on human behaviors and evacuation strategies impact, especially when structural measures fail. This study proposes a multi-step and multi-scale tool, integrating hydrodynamic and evacuation simulations in flood-prone HUBEs, to (1) evaluate how excluding or including human behavior affect risk levels, and then (2) how emergency plan can be optimized, by testing different route choice strategies, to improve human safety. The tool combines microscopic and macroscopic models and is applied to typological HUBEs. Final comparisons with a consolidated model contribute to the tool verification, highlighting how the tool (and its single simulation components) can support decision makers in the analysis of multiple scenario and strategies conditions.

Keywords

Flood risk, Historic Urban Built Environments, Emergency planning, Optimization problems, Simulation model.

1. *Introduction*

In latest years, floods have become one of the most frequent and devastating natural disasters worldwide. Their occurrence is on the rise, with an alarming impact on communities and urban areas. Between 2018 and 2022, Italy alone recorded 170 flood-affected locations, resulting in about 60 fatalities or missing persons and the displacement of over 12,000 people. Such numbers dramatically worsened in 2023, when over 40 cities have been hit by flooding events, leading to nearly 40,000 evacuees and homeless (Bianchi & Salvati, 2024).

Flood risk is particularly critical in urban areas located in riverine settings, floodplains, coastal zones, and nearby dikes. Historic Urban Built Environments (HUBEs) within these areas face even greater vulnerability due to a combination of different factors (Ferreira & Santos, 2020), including climate change, complex and narrow urban layouts, the structural fragility of historical buildings, and poor risk mitigation measures. Additionally, these areas often attract large populations and tourists who may be unfamiliar with the risks, local geography, and emergency procedures, further increasing the potential for risk disaster (Arrighi et al., 2019; Ferreira & Santos, 2020; De Padova et al., 2024).

1.1 *From flood risk assessment to mitigation: basic concepts*

Flood risk, like other disasters, can be defined as the combination of three key factors (UNDRR, 2024). Vulnerability depends on HUBE features such as urban morphology, spatial geometry, construction materials, and proximity to the source of danger that affect both the floodwater spreading and the human response to the event (Ferreira & Santos, 2020; Mignot et al., 2019). Hazard concerns the features of the event such as, in the case of floods, the water speed and depth over space and time, as well as the source of danger (e.g., fluvial, pluvial, or coastal flooding) (Mignot et al., 2019). Human exposure and vulnerability consider aspects such as population density, individual behaviors, and people's capacity to react effectively in emergency situations also in view of factors like physical condition, age, gender, height, mobility, and

decision-making abilities (Arrighi et al., 2019; Dias et al., 2021).

Different strategies could be adopted to mitigate flood risk in HUBEs, but they should be accurately balanced to take into account all the aforementioned factors. Emergency conditions induced by extreme floods may obstruct or prevent the effectiveness of structural solutions, thus implying the necessity of evacuation procedures (Lumbroso & Davison, 2018). These scenarios can include flash floods or any other case in which preventive evacuation procedures (e.g. by car) could not be performed, thus forcing users to eventually move on foot in the flooded HUBEs (Arrighi et al., 2019; Musolino et al., 2022). These procedures include vertical evacuation and shelter-in-place towards upper floors/levels, which can be relevant for building occupants (Lumbroso & Davison, 2018), but could become unfeasible for users placed in outdoors or at the building ground floor due to availability, accessibility, capacities and distance problems (Hsiao et al., 2021). Accordingly, horizontal evacuation could be performed, forcing users to move on foot in the floodwater-affected HUBE to reach predefined or temporary "safe heavens" (Lumbroso et al., 2023; Lumbroso & Davison, 2018). In these circumstances, the risk is widely affected by users' behaviors, motion conditions, interaction with floodwaters and individual/group decision-making toward the identification and selection of shelters and evacuation routes (Lumbroso et al., 2023).

Focusing on floodwater effects on pedestrian motion features, they can lead to instability, reduced movement speed, and deviations in trajectory (Cox & Shand, T.D.Blacka, 2010; Quagliarini et al., 2022). In particular, according to established literature (Cox & Shand, T.D.Blacka, 2010), critical local floodwater depth D [m] and speed V [m/s] can be used to evaluate maximum stability thresholds for adult pedestrians[1] (i.e. D>1.2m, V>1.2m/s, and DV>1.2m/s^2). Furthermore, the maximum evacuation speed can be determined according to equation (1), where g=9.8m/s^2 is the gravitational acceleration:

$$V_p = 0.5\left(\frac{D\cdot V^2}{g}+\frac{D^2}{2}\right)^{-0.1} \quad (1)$$

1.2 The contribution of simulation tools

Digital technologies can support the process of risk assessment and mitigation, providing reliable tools for the representation, management and simulation of different conditions of the HUBEs, including those related to the application of non-structural strategies. In particular, similar to other kinds of disasters (e.g. fire) (Ronchi, 2021), evacuation simulators represent a trade-off between accuracy and scalability, and present significant advantages over real-life experiments with actual participants (e.g., difficulty in setting up realistic conditions, exposing participants to significant danger).

In fact, simulation tools are becoming increasingly important, and different models have been introduced as decision-support tools for designing, managing, and evaluating evacuation safety and efficiency (Evans et al., 2024; Zhuo & Han, 2020). Nevertheless, although they offer a sustainable strategy to improve evacuation plans in HUBEs, the paramount role of human behavior in flood risk assessment and mitigation seems to be still limitedly explored (Lumbroso et al., 2023; Musolino et al., 2022). One of the most challenging issues in this context is the optimal allocation of pedestrians to predetermined evacuation routes and shelters. Addressing these complexities requires digital tools and validated simulation models that aid safety designers in risk management, assessment and planning (Lumbroso et al., 2023; Zhuo & Han, 2020).

When determining the optimal location of shelters, key factors typically include altitude, number, capacity, distance from sources of danger, or a combination of them through multicriteria decision analysis (Hsiao et al., 2021; Lee et al., 2020). Furthermore, since survival probability, evacuation time, and evacuation distance are among the most important factors influencing disaster response, minimizing these parameters plays a key role in identifying optimal evacuation routes (Ma et al., 2019).

To address such issues, current methodologies can use two different simulation approaches differentiated by their modeling scale, namely microscopic and macroscopic (Beyki et al., 2023; Chraibi et al., 2018; Spearpoint et al., 2024).

[1] Pedestrians with a mass per height higher than 50 [kg·m]

1.3 Microscopic models

Microscopic models consider each pedestrian individual properties (e.g., walking speed, destination, position, decision-making behaviors), and local interactions with other pedestrians, built environment, and floodwaters (Chraibi et al., 2018; Lumbroso & Davison, 2018). Accordingly, these models are useful to plan and design specific interventions to improve HUBEs safety and functionality at a local-scale (Bernardini et al., 2021; Lumbroso et al., 2023). They provide reliable, fine-graded insights also for scenarios with many pedestrians who, differently from macroscopic approaches, move according to local optimal decisions (i.e., pedestrian are not fully aware of the overall scenario (Borrmann et al., 2012)). However, due to their high level of detail and accuracy, microscopic models can be impacted by lower computational performance and higher effort to set up scenarios than macroscopic models.

Typical microscopic models include cellular automata (Li et al., 2019), force-based models (Helbing & Molnár, 1995), and agent-based models (Zhuo & Han, 2020). The latter, in particular, allows a thorough evaluation of the interactions of pedestrians with surrounding buildings, vehicles, floodwaters, and how damage conditions evolving over time (Lumbroso et al., 2023). Previous research also integrates "social" forces into agent-based modeling, describing individual interactions with the surrounding environment by mean of repulsive forces (e.g. to avoid collisions with obstacles and other pedestrians) and attractive forces (e.g. towards a desired destination) (Helbing & Molnár, 1995; Quagliarini et al., 2022). As a result, each agent has desired speed and direction evolving dynamically, that depend on its own goal and interactions (thus including others' behaviors). Stochastic elements to account for inherent uncertainties and variations in human behavior over time and space can be included, thus improving realism while needing a statistically-based assessment of outcomes (Jiang et al., 2020). This kind of application can also include reliable simulation of significant crowd conditions in floodwaters (Liu & Lim, 2018).

However, the possibility to exploit these models should be balanced in terms of collection, management and interpretation of input data, simulation variables, and outputs, especially considering the application by technicians with medium-low level of expertise on the modelling of pedestrian behaviors (Quagliarini et al., 2022) and the need for high computational resources, especially in complex scenarios involving large populations (Z. Zhu et al., 2018). This slows down simulations and makes them challenging to scale, as they require detailed input data and demand significant user effort. In this sense, "the uncertainties associated with the inputs may be more significant than the certainties associated with the model output" (Spearpoint et al., 2024), thus increasing the complexity, for practitioners, to deal with simulation inputs, criteria and outputs (including their interpretation) in an effective and clear manner.

1.4 Macroscopic models

Macroscopic models are mainly based on optimization approaches representing pedestrians as homogeneous groups sharing features and following supervised decisions (Chraibi et al., 2018; Hamacher & Tjandra, 2002). Accordingly, they can be used to compute conservative estimations in aggregate quantities (e.g., densities, speeds, times), and are suitable especially for large-scale scenarios with complex geometries (Borrmann et al., 2012; Hamacher & Tjandra, 2002) and low-density conditions involving few interactions between pedestrians (e.g., when bidirectional flows are unexpected) (Bayram, 2016; Bayram & Yaman, 2018). In this sense, they are able to focus on strategic decision support (Carrozzino et al., 2012; Huertas et al., 2020).

Evacuation routing can be done along graphs representing the scenarios and their features in static networks composed of nodes and arcs measuring, for instance, times, distances, and/or other different costs (Hamacher & Tjandra, 2002). Specifically, network flow mathematical programming models typically prescribe how flows of goods, information, or general entities move in the network according to well-defined hypotheses and constraints. For instance, in the context of floods, classic approaches rely on the evaluation of the shortest distance (Guo et al., 2018) or the shortest time (Y. Zhu et al., 2022), but there are still actual uncertainties (especially at the urban scale) about the best route selection policy (e.g., shortest, quickest, or less effortful).

Most of the mathematical formulations proposed in the literature decompose location and evacuation decisions into sequential steps to

simplify the computation of solutions, thus representing a viable solution in terms of operative sustainability, but at the cost of potential suboptimal results. On the other hand, the much harder integrated problem of optimally selecting the number and location of shelters and concurrently defining the related evacuation routes is addressed in the literature by only a few models (Bayram, 2016) mostly relying either on single-level modeling (i.e., multi-objective mixed-integer linear programming approach (Coutinho-Rodrigues et al., 2012), second-order cone programming, or nonlinear modeling (Bayram & Yaman, 2018)), or on bilevel programming (generally harder to solve, and whose solutions are often left to heuristics (Dempe et al., 2015)).

In general, although less detailed in simulating individual behaviors, macroscopic models are generally characterized by a higher scalability level, higher computational efficiency and, at the same time, lower level of details in terms of scenario modelling about buildings, users, and hazards, making them exceptionally suitable for scenarios involving large populations and complex environments.

1.5 Work aims

Three main novel aspects are introduced in this work: (i) the integration of a multi-scale perspective into evacuation modeling and into the optimization of shelter allocation and evacuation routes; (ii) the adoption of a multi-criteria optimization process, enabling informative and multipurpose risk indicators; and (iii) the validation of the proposed framework through comparison with a well-established microscopic simulator (Life Safety Model (Evans et al., 2024; Lumbroso et al., 2023)), moving towards tool verification. These points, at the best of the authors knowledge, address gaps still underexplored in current literature (Bashir et al., 2025; Lopes et al., 2025). Consolidated HUBE layouts are used as a case study to demonstrate the proposed novel framework (Bernardini et al., 2021).

Starting from these premises, the work also addresses risk variations depending on whether human behavior is evaluated or not in the analysis, to optimize evacuation planning in flood-prone HUBEs. To achieve this goal, specific tools are defined and combined, and new metrics are introduced to quantify the impact of pedestrian dynamics on flood risk. About simulation tools, hydrodynamic simulation is combined with multi-scale approaches, leveraging the advantages of: (1) microscopic models in understanding the effects of human behaviors in flood risk evaluation; and (2) macroscopic models in boosting optimization tasks for evacuation strategies definition. On this basis, developed metrics enable comprehensive, holistic, and multi-level analyses through rapid, data-driven assessments.

Results provide systematic comparisons across different urban layouts, evacuation strategies, environmental conditions, and simulation models within a unified framework, ensuring a robust evaluation of flood risk and evacuation efficiency. Additionally, high-risk areas within specific scenarios can be identified, supporting targeted risk mitigation strategies. By leveraging these insights, decision-makers can enhance shelter placement, optimize evacuation routes, and evaluate the effectiveness of different response strategies, improving urban resilience against flood hazard.

2. Phases, materials and method

The work is organized according to the general methodology outline shown also inFig. 1, on which this Section is also structured. The workflow is applied with respect to six typological HUBEs traced according to recurring features in the Italian context, as shown in Section 2.1.

Key Performance Indicators (KPIs) for flood risk assessment and their combination into two Risk Indexes (RIs) have been first defined, assuming that they can vary on a common scale [0-1], as discussed in Section 2.2. KPIs are aimed at enabling fair and systematic comparisons across multiple dimensions (i.e., different evacuation layouts, strategies, behavioral assumptions and related modeling approaches). The first Risk Index excludes the impact of behaviors from risk assessment (RI_{EB}) relying solely on hydrodynamic simulation performed according to Section 2.3. The second Risk Index includes behavioral factors (RI_{IB}), combining hydrodynamic simulations with behavioral evacuation simulation outputs. In particular, evacuation simulations are performed using a microscopic (Section 2.4) and a macroscopic (Section 2.5) model, ensuring a robust, multi-scale application process. A third well-established microscopic model (Section 2.6) is finally considered for verification purposes.

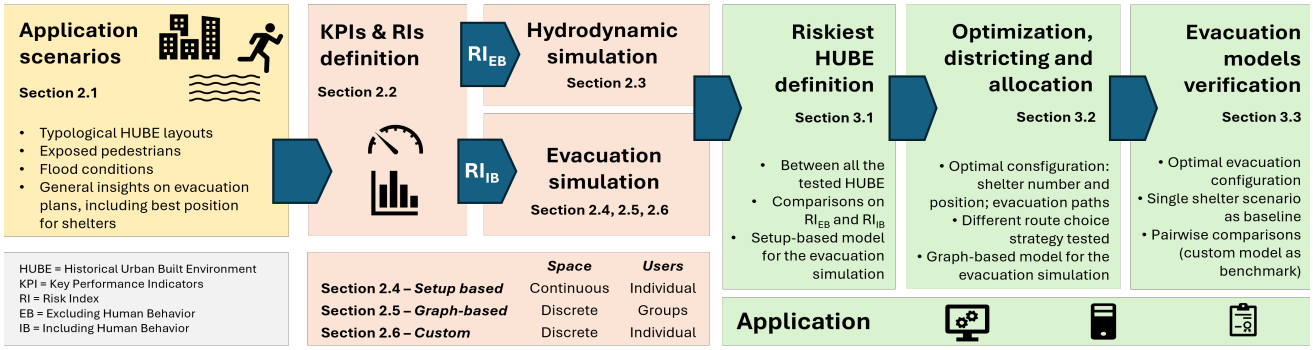

Fig. 1: Graphical framework.

RI_{EB} and RI_{IB} are exploited in the following tasks in the typological HUBEs contexts, according to the application purposes defined in Section 2.2. First, they are used to determine the most critical scenario among the considered HUBEs, allowing for a systematic assessment of flood risk excluding and including human behavior impact. In particular, RI_{IB} essentially relies on basic configurations for evacuation dynamics, i.e., considering as N potential shelters as the dry or quasi-dry areas (i.e., DV<0.6 m^2/s to minimize the interaction between users and floodwaters (Bernardini et al., 2021)), and assuming the users just select the nearest available area. To ensure detailed results on RI_{IB}, the microscopic model defined in Section 2.4 has been employed. Results of this first task are reported in Section 3.1.

Then, the riskiest HUBE is selected for determining the optimal configuration in terms of shelters number and position, as well as the safest evacuation routes to reach them. Additional criteria on human behavior for path choice are also comprised, exploiting the macroscopic model introduced in Section 2.5. This choice is driven by the model's ability to efficiently process all the possible Ω combinations, determined according to Equation (2):

$$\Omega = h \cdot i \cdot \sum_{k=1}^{N} \binom{N}{k} \quad (2)$$

where h is the number of HUBEs (in this work h=1, i.e., the most critical one), N is the number of potential shelter locations to be considered (ranging from 1 to) and i is the number of route choice strategies (e.g., the shortest, the fastest, the less effortful (Guo et al., 2018; Y. Zhu et al., 2022)). To this end, mathematical programming techniques, such as optimization algorithms, are employed to significantly reduce computational time and ensure faster results, making it more suitable for handling large-scale simulations compared to microscopic models. Optimization criteria include the minimization of the number of casualties, in combination with length, time, or pedestrian evacuation effort with respect to the overall number of pedestrians involved (Guo et al., 2018; Y. Zhu et al., 2022). In detail, the proposed model relies on validated techniques (i.e. Integer Linear Programming, ILP) applied for the first time to flood pedestrian evacuation. Results of this second task are reported in Section 3.2.

Finally, the optimal evacuation configuration is further simulated using the well-established flood evacuation simulator introduced in Section 2.6, for verification purposes, using the related evacuation simulation outputs into RI_{IB}, to ensure reliability and consistency in comparisons. This simulator was selected for its shared features between the other two models. In particular, it shares the individual-based representation of pedestrians with the microscopic model, accounting for their unique characteristics, while it shares the discretization of space with the macroscopic one, representing the environment as a network of nodes and links. This approach enables, for the first time, a cross-comparison between these three approaches, providing deeper insights into their performance differences. Results of this task are reported in Section 3.3.

2.1 Application scenarios

The application scenarios consider typical conditions observed in riverine HUBEs across Italy. To analyze these patterns, different urban areas affected by major floods in recent decades[2].

[2] Albenga (SV) in 1994, Carrara (MS) in 2003, Colorno (PR) in 2017, Montevarchi (AR) in 1966, and Senigallia (AN) in 1976, 2014, and 2022.

were selected as case studies. Building on findings from a previous study, this analysis explored key urban features, including the orientation of streets in relation to the river's main flow direction, the average width and slope of the streets, the average size of building blocks, the presence of squares, as well as the features of the fluvial flooding to be simulated (Bernardini et al., 2021).

This analysis led to the identification of six HUBE typologies. Five of these include a street network oriented perpendicularly to the river, differing primarily in the placement and dimensions of squares, which range from one to two building blocks. The sixth typology does not include a square. Fig. 2 illustrates their layouts, while Tab. 1 provides a summary of their geometrical features.

Tab. 1: Features of the streets composing the HUBEs. Squares can be composed of 1 or 2 building blocks.

	Width	Length	Slope
Streets parallel to the river	4.0 m	33.0 m	0.3%
Streets parallel to the river	6.0 m	67.0 m	0.6%
Building blocks	33.0 m	67.0 m	-

For all the configurations tested, a population of 240 adult pedestrians homogeneously distributed in each of the outdoor area of the HUBEs is considered according to low density conditions typical of possible flood evacuation scenarios (i.e., 0.18 persons/m^2 (Bloomberg & Burden, 2006)).

2.2 KPI and RI definition

Simulation analyses were conducted at two distinct levels: 1) hydrodynamic modeling, to assess only floodwater hydrodynamics and 2) evacuation modeling, to evaluate pedestrian movement and safety factors. Based on the simulation outputs, two distinct Risk Indexes are defined: the first one is derived only from hydrodynamic analysis and excludes human behaviors (RI_{EB} [-]); the second one is obtained from the evacuation simulations and includes also human behavior insights (RI_{IB} [-]). The simulation outputs are first structured into a set of Key Performance Indicators (KPIs), then integrated into the Risk Indexes.

Tab. 2 presents an overview of the selected KPIs and their corresponding calculation methods. To ensure consistency in normalization, a conservative approach is adopted, as the maximum values for each metric are considered (Bernardini et al., 2021). The KPIs and the RIs are standardized on a scale from 0 to 1, with 0 indicating no risk and 1 representing the highest level of risk.

The RIs calculation (Eq. 3) is formulated using the Euclidean norm of a vector in a *p*-dimensional space, where *p* corresponds to the number of Key Performance Indicators (KPIs) considered.

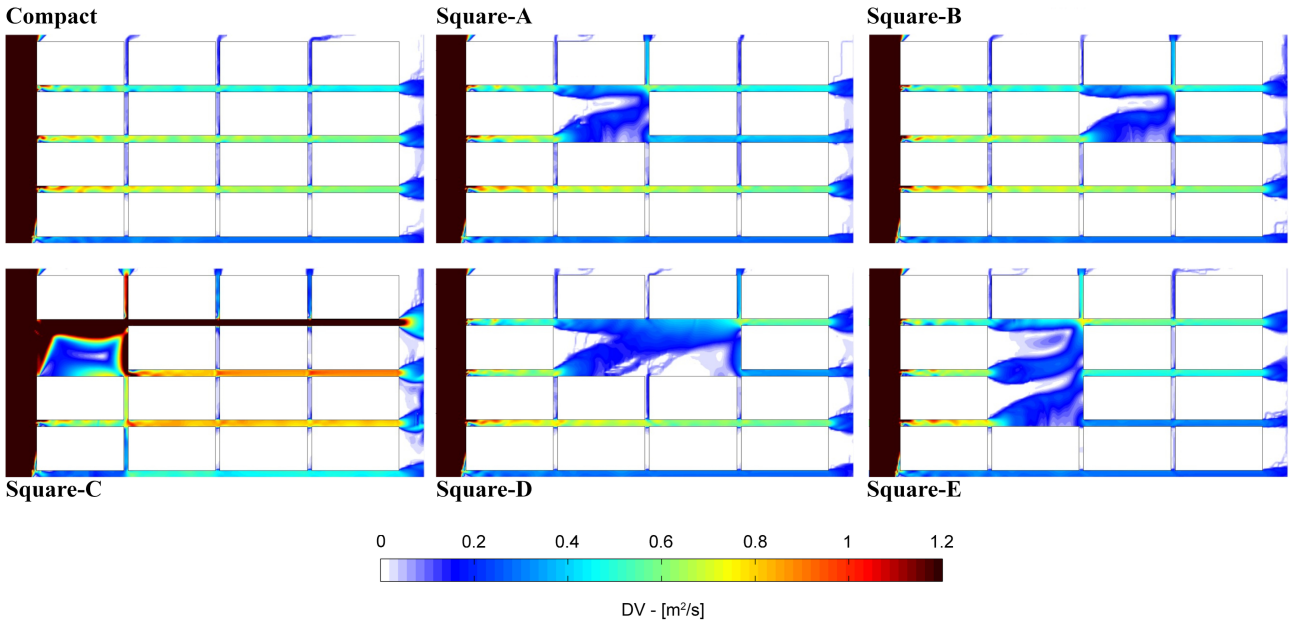

Fig. 2: Maps of the typological HUBEs (white rectangles represent building blocks) and the floodwater hydrodynamic conditions evaluated in terms of DV during the event peak time [m^2/s].

$$RI = \sqrt{\frac{\sum_{k=1}^{p} W_k^2 \cdot KPI_k^2}{\sum_{k=1}^{5} W_k^2 \cdot 1^2}} \quad (3)$$

For the hydrodynamic-based index (RI_{EB}) the calculation involves a single KPI concerning with the stability of exposed users in the HUBEs (p=1, as shown in Tab. 2a). In contrast, the evacuation-based index (RI_{IB}), which integrates evacuation simulation results and accounts for human behaviors, is derived from four KPIs (p=4, as shown in Tab. 2b). To ensure a balanced representation of each factor in the RI_{IB} computation, the Analytic Hierarchy Process (AHP) has been employed to determine the relative importance of the KPIs through pairwise comparisons (Saaty, 1980). This approach assigns weighting coefficients (W_K) to each KPI, quantifying the contribution to the overall risk assessment. Among the KPIs evaluated for the evacuation-based assessment, the missing pedestrian ratio has been identified as the most critical indicator.

RI_{EB} and RI_{IB} are calculated for each typological HUBE to better highlight the impact of human behavior on the overall risk. Specifically, these indexes allow addressing three key aspects:

1. **Definition of the riskiest HUBE**. This is achieved by comparing the results of RI_{EB} and RI_{IB}, under different HUBE conditions (in this case, same hazard and floodwater spreading inputs, but different layouts) allowing for an objective assessment of flood risk with and without considering human behavior. These concepts are applied to results in Section 3.1;
2. **Assessment of the optimal evacuation configuration**. This implies evaluating the optimal solution in terms of number and position of shelters and evacuation routes according to RI_{IB} results. These concepts are applied to results in Section 3.2;
3. **Model validation**. Cross comparisons are performed in the selected HUBE, evaluating both the optimal and the riskiest configuration (as best- and worst-case scenarios) based on KPIs and RI_{IB} results. These concepts are applied to results in Section 3.3.

2.3 Hydrodynamic simulation

The hydrodynamic simulation was performed with the open-source software Delft3D (v4.03.013, available at https://oss.deltares.nl/web/delft3d/downloads, last access on 29/05/2025), which employs a 1m × 1m computational grid for the outdoor spaces of the HUBEs. This tool provides water depth D, speed V, and their product DV values for each grid

Tab. 2: KPI calculation methods and their definitions organized by Risk Index (RI_{EB} in Table 2a, which is excluding human behaviors, and RI_{IB} in Table 2b, which is including human behaviors).

KPI	Definition	Calculation method	W_K	Simulation [RI]
idv	Normalized stability index	$\min(DV_{i,j}/1.20, 1)$, where $DV_{i,j}$ is the average DV weighted by outdoor areas ($\sum DV \cdot A / \sum A$, being A the area of each street and square of the HUBEs), and 1.20 is the maximum DV stability threshold	1	Hydrodynamic [RI_{EB}]

KPI	Definition	Calculation method	W_K	Simulation [RI]
s	Normalized evacuation length	$S_{AVG(i)}/ \max_{(i)}\lvert S_{AVG(i)}\rvert$ average evacuation length traveled by pedestrian to reach shelter normalized with respect to its maximum value considering all the tested configuration	0.2	Evacuation [RI_{IB}]
t	Normalized evacuation time	$T_{AVG(i)}/ \max_{(i)}\lvert T_{AVG(i)}\rvert$ average evacuation time spent by pedestrian to reach shelter normalized with respect to its maximum value considering all the tested configuration	0.2	Evacuation [RI_{IB}]
dvs	Normalized evacuation effort	$DVS_{AVG(i)}/ \max_{(i)}\lvert DVS_{AVG(i)}\rvert$ average evacuation effort spent by pedestrian to reach shelter normalized with respect to its maximum value considering all the tested configuration	0.2	Evacuation [RI_{IB}]
mp	Missing pedestrian ratio	$Z_{(i)}$ / 240 ratio between pedestrians unable to reach shelter and overall number of pedestrians taking part in the evacuation	0.4	Evacuation [RI_{IB}]

cell at 60-second intervals. The hydrodynamic conditions are evaluated in the noticeable points of the six HUBEs (i.e., barycenters and vertices of streets and squares), using a reliable discretization according to homogeneous values of maximum local values of *D, V,* and *DV* gained at the event peak time (Bernardini et al., 2021). These parameters are then used to derive effects on pedestrian motion in terms of stability and maximum speed, according to criteria introduced in Section 1.1 (see also Equation 1). The floodwaters conditions are based on a reference riverine flood with a return time of 100 years and a maximum flow rate Q = 1148 m³/s (Bernardini et al., 2021).

2.4 Setup-based model

The first microscopic model tested relies on a setup-based version of Oasys MassMotion (v11.0.13, available at https://www.oasys-software.com/products/massmotion/, last access on 25/09/2025), a generic commercial software for crowd modeling in non-flooded conditions. This model has been recently adapted also for flood-related evacuation thanks to specific setup with no-source code modifications (Bernardini et al., 2021). This model exploits a social force-based approach and the adopted setup have been verified by previous research activities through comparisons with real-world data and a custom flood evacuation simulator (Quagliarini et al., 2022). Pedestrians are randomly distributed in the HUBEs to meet the aforementioned crowding conditions (i.e., no specific position is assigned to each pedestrian). Furthermore, V_p depends on D and V conditions according to Section 1.1 criteria, but they can also decrease due to simulated interactions with other pedestrians and the surrounding built environment, since microscopic groups dynamics are modelled by means of the social forces. In this model, pedestrians move continuously in space (i.e., outdoor areas, also enabling a complete 3D representation) and time, also allowing local assessments on single pedestrians having their own trajectories and preferred speed.

2.5 Graph-based model

The proposed macroscopic model is based on an oriented graph representation of the street networks of the idealized HUBEs.

Fig. 3 shows an example calibrated on scenario "Square C": the starting points are indicated by the black and red nodes, while the overall potential shelters only by the red nodes (Bernardini et al., 2021). In other words, of all the nodes that compose the graph, only the red ones can be both starting points and shelters as nodes represent HUBE outdoor areas.

Green lines in

Fig. 3 represent links as segment of paths. A link could be a street or a part of a square. Pedestrians are only allowed to move away from the source of risk (i.e., the river), thus links parallel to the river are not oriented and can only be traveled in both directions, while perpendicular and oblique links (which are fictitiously include to model the square into sub-areas) are oriented and can only be traveled downstream (away from the river) (Bernardini et al., 2021). Exceptions to these rules occur when moving upstream is the only way to stay in testing scenario, i.e., in the streets furthest from the river.

Pedestrian maximum speed and stability are modeled by associating costs to each link of the graph through the relationships introduced in Section 1.1. Links with D≥1.20m, V≥3.00m/s, or DV≥1.20m²/s cannot be traveled (Cox & Shand, T.D.Blacka, 2010), according to criteria for pedestrian stability.

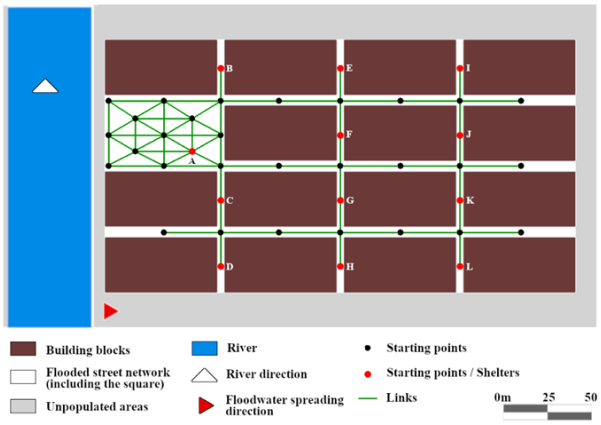

Fig. 3: Example of the graph used to represent the street network on scenario "Square-C" (Bernardini et al., 2021): black nodes indicate the evacuation starting points, red nodes can be both starting points and shelters (i.e., evacuation ending points). Green lines indicate the links between the nodes

Three different evacuation strategy i for the pedestrian route choice (i.e., the shortest, the quickest or the cheapest, resumed in Tab. 3 together with their computation method) are

tested in the macroscopic model by varying the number of available shelter *N* (i.e., from 1 to 12).

Tab. 3: Evacuation strategies for the route choice and their computation method depending on the link cost.

i	Route choice strategy	Minimized parameter	Link cost *c*
s	Shortest	Evac. length	*S* [m]
q	Quickest	Evac. time	*T* [s]
c	Cheapest	Evac. effort	*DV·S* [m³/s]

Therefore, 36 different optimal scenarios amongst *i,N* combinations are simulated. For each scenario, the optimal solution is computed through the minimization of the number of casualties together with the impact of human behavior effects on path choices in terms of, respectively, the sum of the: evacuation length for the "shortest" strategy; evacuation time for the "quickest" strategy; and effort for the "cheapest" strategy.

In particular, the objective function minimizes the total number of pedestrians rather than the more disadvantaged single pedestrian, thus rewarding the group dynamics than individual ones. This way, the model assumes that a single pedestrian could accept a difficult evacuation route if this choice helps many other pedestrians. Each optimal solution includes the selection of shelters and the evacuation route from the starting nodes to the shelters for each pedestrian, the number of pedestrians unable to complete the evacuation $Z_{(i,N)}$, and an array $\boldsymbol{C}_{AVG(i,N)} = [S_{AVG}; T_{AVG}; DVS_{AVG}]_{(i,N)}$ listing the mean cost values evaluated with respect to successful evacuations. The minimum cost paths on the graph are formulated as an Integer Linear Program (ILP) and solved through the commercial package IBM-CPLEX. The ILP models the case where a single decision-maker (the coordinator of the evacuation operations) computes evacuation routes in a centralized fashion and assigns them to pedestrians (Marinelli, Pizzuti, Romano, Bernardini, & Quagliarini, 2025).

2.6 Custom model

The second microscopic model tested it the Life Safety Model (LSM v3.2, available at https://lifesafetymodel.net/download-lsm/, last access on 25/09/2025), selected in view of its consolidated use in many applications for risk assessment and mitigation via emergency plans for floods and dams (Evans et al., 2024; Lumbroso et al., 2023; Lumbroso & Davison, 2018). From an operational standpoint, LSM is an agent-based model that jointly considers data on hydrodynamics, people/buildings/vehicles and associated behavioral issues, road network, shelters and flood warnings dissemination over space, in a unique tool, and can both estimate losses (of, i.e., people's lives, buildings, vehicles) during time and the evacuation times for people moving on foot. The setup of the LSM for this study has been modeled according to suggested standards from guidelines (HR Wallingford Ltd, 2021). In particular, pedestrians (PARU according to the LSM) are divided into groups (PARG) which correspond (in number and position) to the starting points of the macroscopic model and divided into groups (PARG) which correspond (in number and position) to the starting points of the macroscopic model. To ensure applying the same behavioral parameters of the other microscopic and macroscopic models, healthy pedestrians are modelled considering average initial physical conditions (PPC=1) declining to 0 in 1 hour due to the fatigue of moving into floodwaters (which means that they could survive for about 1 hour within floodwaters). Assigned evacuation speed V_p is about 0.8m/s, which is consistent with about most of the reference hydrodynamic conditions along the available street network (Bernardini et al., 2021), considering that the model does not allow to directly increase speed again once experienced *D* and *V* levels decrease. *DV* toppling criteria, that lead pedestrians to be at least injured by flood, have been associated with 1.2m²/s to ensure consistency with the other models. Pedestrians "are constrained to move" along the road network (which has been setup as in the macroscopic model), according to "travelling cost" approach "which produces the 'least expensive' route for each agent" towards the selected shelters (safe heavens with an individual capacity of 250 people so as to ensure that all the pedestrians can gather in them). "Pedestrians may pass each other while travelling on roads. The pedestrian density on the network is not a factor in the model" (Lumbroso et al., 2023).

3. Results

This section presents the results in a structured manner, following Fig. 1 framework and the application of tools and RIs defined in Section 2.2. First, the riskiest HUBE is determined (Section

3.1), then the macroscopic model is applied to this layout to test the districting and optimization of shelters and evacuation paths (Section 3.2). Finally, the three different evacuation modeling approaches are tested and compared based on the optimal evacuation configuration (Section 3.3). The assessments are conducted through the risk indexes RI_{EB} and $RI^{A}_{IB(i,N)}$ introduced in Section 2.2, using the following notation: the superscript *A* indicates the reference simulation model (*g* stands for the macroscopic graph-based model, *lsm* stands for the custom model, *mm* stands for the microscopic setup-based), *i* indicates the evacuation route choice strategy affecting human behavior (see Tab. 3) and *N* indicates the available shelters number.

3.1 Determining the riskiest HUBE

Results shown in Tab. 4 offer general insights into the typological HUBEs, which can represent different aligned layout configurations, based on the hydrodynamic risk index (RI_{EB}) and the evacuation risk index (RI_{IB}).

Tab. 4: Evaluation of the riskiest HUBE through the hydrodynamic (RI_{EB}) and the evacuation (RI_{IB}) risk indexes.

HUBE	RI_{EB}	RI_{IB}
Compact	0.54	0.16
Square A	0.41	0.12
Square B	0.42	0.12
Square C	*0.82*	*0.46*
Square D	0.35	0.09
Square E	0.34	0.12

Overall, the results indicate that including user dynamics in flood risk assessment leads to notable differences in the selected case studies. Specifically, in all the tested scenarios, excluding human behavior in flood risk assessment (see RI_{EB}) could lead to very conservative outcomes, which could be not consistent with the effective safety of hosted population, which can effectively apply safe strategies by reaching the gathering points. In fact, according to Table 2, RI_{EB} just comprises the effects of floodwaters spreading on human stability through *idv*, ignoring the detailed effects in the evacuation process which are included by the KPIs on which RI_{IB} is defined. Furthermore, when analyzing specific risk conditions, the presence of a square adjacent to the river increases the flood risk as the floodwaters soak in the HUBE without obstruction from building blocks (i.e., Square C), thus increasing pedestrian slowdowns, stability loss, and casualties due to more hazardous hydrodynamic conditions. Moreover, the compact layout appears more vulnerable than scenarios including a square within the built environment (i.e., case studies A and B), especially as the square size increases (i.e., case studies D and E).

However, since the evacuation simulations assume the presence of shelters in all dry or quasi-dry zones (that in the proposed HUBEs are placed in the middle point of the streets parallel to the river and downstream parts of the squares, as shown in Fig. 2), further evaluations should be conducted to assess whether it is possible to streamline the number of shelters without affecting risk levels. In particular, the proposed optimization framework determines the optimal number and positioning of shelters together with the best path to reach them by considering three different evacuation strategies, namely the shortest, the quickest, and the cheapest path. Given the results obtained, the Square C case study has been selected for this purpose, considering its particularly high-risk conditions and the challenges it poses for evacuation dynamics.

3.2 Optimizing shelters and evacuation paths

The optimal number of shelters to be provided in the selected HUBE (Square C) is evaluated by analyzing $RI^{g}_{IB(i,N)}$ trends, summarized in Fig. 4.

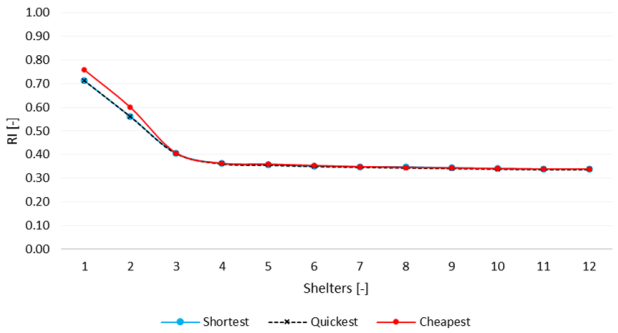

Fig. 4: $RI^{g}_{IB(i,N)}$ values depending on the evacuation strategy route choice *i* and the number of shelters available *N*. "Shortest" and "quickest" trends are overlapped.

Evacuation strategies involving one and two available shelters are the riskiest ones. The *cheapest* strategy in route choice exposes pedestrians to travel greater evacuation lengths (S) and times (T) to obtain benefits in terms of effort (DVS), thus increasing the overall risk ($RI^{g}_{c,1}$

and $RI^{g}_{c,2}$). The risk slightly decreases with the *shortest* and the *quickest* strategies ($RI^{g}_{s,N}$ and $RI^{g}_{q,N}$ are overlapped), until moving towards results convergence at three available shelters, thus identifying a threshold beyond which the risk no longer varies with the evacuation strategy and the shelters' positions. However, it can be noticed that with more than four shelters, $RI^{g}_{l,N}$ does not significantly decrease (i.e., $RI^{g}_{l,4}$= 0.36, and it drops by less than 5% by adding supplementary shelters), thus identifying the optimal number of shelters for risk reduction. Accordingly, considering four shelters, Fig. 5 shows their unanimous (i.e., agreed with the three strategies tested) optimal positioning (red pinned nodes *K, A, G,* and *D*), the evacuation routes to reach them, and the following districting in evacuation units (i.e., basic sectors that include at least a shelter and the evacuation routes to reach it).

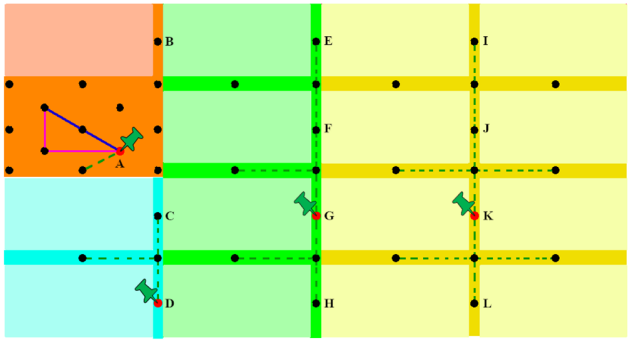

Fig. 5: Shelters position and evacuation routes to reach them with *N*=4. Non-linked nodes are deadly points. Green dashed lines indicate evacuation routes shared with the three strategies, magenta lines shared with "shortest" and "quickest", blue lines for "cheapest".

Tab. 5: Shelters selection depending on the route choice strategy and the number of shelters available (only configurations with *N*≤4).

Strategy	***N*=4**	***N*=3**	***N*=2**	***N*=1**
Shortest (*i*=s)	K; A; G; D	K; A; G	K; A	K
Quickest (*i*=q)	K; A; G; D	K; A; G	K; A	K
Cheapest (*i*=c)	K; A; G; D	K; A; G	L; A	L

The shelters positioning in Fig. 5 shows how the optimal solution exploits the shielding provided by the building blocks according to a "modular" criterion, that is every street parallel to the river (therefore every 66m). To this end, Tab. 5 also shows that even decreasing the number of available shelters, at least one of them should be placed in the street furthest from the river (shelters *K* and *L*), and the other one in the square, since shelter *A* is the only one that manage to reduce the number of pedestrians unable to complete the evacuation $Z^{g}_{(i,N)}$ due to the hydrodynamic conditions in the corner nodes of the square that prevent moving toward the streets (deadly points are represented by non-linked nodes in Fig. 5).

For what concerns the path selection behaviors, results shows that the possible evacuation strategies provided the same evacuation routes to reach the shelters located along the streets (green dashed lines in Fig. 5). Indeed, to reach the shelter in the square, the "cheapest" strategy (blue solid lines) slightly differs from the "shortest" and the "quickest" ones (magenta solid lines). Nevertheless, all the strategies are characterized by the same level of risk ($RI^{g}_{i,4}$= 0.36). Therefore, limited differences in human behavior about path choice are retrieved.

Tab. 6 finally summarizes the number of pedestrians supposed to move inside each evacuation unit and the following number of pedestrians expected to be allocated, evaluated excluding the number $Z^{g}_{(i,N)}$ of pedestrians unable to complete the evacuation due to their starting position in deadly nodes (88 pp). It is worth noticing that, except for *N*=1, $Z^{g}_{(i,N)}$ cannot be decreased due to the hydrodynamic conditions within the HUBE, regardless of the evacuation strategies and the number of shelters arranged.

Tab. 6: Number of pedestrians present and to be allocated in each evacuation unit. Their difference is the number of pedestrians unable to complete the evacuation in each evacuation unit.

Shelter	**Evac. unit**	**Ped. present**	**Ped. to be allocated**
K	Yellow	82	60
G	Green	49	38
D	Blue	19	19
A	Orange	90	35
All	All	240	152

3.3 Comparing simulation models

Comparisons are performed according to the best evacuation configuration from Section 3.2 (i.e. *N*=4) and to the worst ones (i.e., *N*=1, thus referring to single shelter scenarios exploited for normalization purposes). Given the route choice

Tab. 7: Comparison between the best evacuation configuration KPIs of the different modeling approaches. The subscript *i* has been removed from the KPIs and RI_{IB} since no differences emerged between the three route choice strategies considering the optimal configuration. *: the difference is calculated with respect to the overall initial number of pedestrians (240 pp).

Modeling approach	$Z^A_{AVG(4)}$	mp^A_4	$S^A_{AVG(4)}$	s^A_4	$T^A_{AVG(4)}$	t^A_4	$DVS^A_{AVG(4)}$	dvs^A_4	$RI^A_{HB(4)}$
Graph-based	88	*0.37*	42	*0.37*	66	*0.37*	19.2	*0.31*	**0.36**
Life Safety Model	89	*0.37*	47	*0.41*	64	*0.44*	22.5	*0.39*	**0.39**
Setup-based	103	*0.43*	33	*0.34*	52	*0.34*	19.6	*0.31*	**0.39**
Percentage differences									
Graph-based vs LSM	0%*	*0%**	-11%	*-9%*	3%	*-16%*	-15%	*-21%*	**-7.5%**
Graph-based vs setup-based	-6%*	*-6%**	+27%	*+8%*	+27%	*+8%*	-2%	*0%*	**-8%**
Setup-based vs LSM	+6%*	*+6%**	-30%	*-16%*	-19%	*-22%*	-13%	*21%*	**0%**

criteria, according to which the three tested strategies can be considered equivalent in the optimal configuration, the subscript *i* has been removed from the KPI and RI in Tab. 7, as the results can be generalized.

Focusing on single KPIs results, the missing pedestrians' ratio (mp_4), evaluated with respect to the total population taking part in the evacuation, shows the adherence between the macroscopic and LSM results, while the microscopic setup-based model slightly overestimates the impact of flood conditions on pedestrian safety. Nevertheless, percentage differences due to this approach is in line with relevant literature acceptability thresholds of 15 to 20% for differences due to the modeling logics at both macroscale and microscale (Quagliarini et al., 2022). Main differences can be due to the starting positions in the microscopic setup-based model, which considers pedestrians distributed on an outdoor area rather than placed at a single node (as for macroscopic and LSM approaches, indeed)

The normalized average evacuation length (s_4) calculated through the macroscopic model is closer to the LSM (9% lower) than the microscopic setup-based model (8% higher). Nevertheless, such differences correspond, in absolute terms ($S_{AVG,4}$), to less than 15m considering the most distant values (i.e., LSM vs microscopic setup-based), which is consistent with the slight differences in the starting positions and the pedestrian interactions of the two models. Considering this KPI, differences between the microscopic setup-based model and LSM are the most relevant, although they are still acceptable in respect to the literature acceptability threshold.

The normalized average evacuation time (t_4) follows the same trend of s_4. Therefore, the macroscopic and the LSM outcomes are closer and lower than the literature acceptability threshold, while the microscopic setup-based approach is characterized by the lowest values. Differences in percentage are mainly due to the normalization values obtained with only one shelter. In view of the above, it is worth noting that, although the percentage differences between the microscopic setup-based model and LSM are slightly over the literature acceptability threshold, differences in absolute terms ($T_{AVG,4}$) for all the tested approaches are quite limited and differ of only 15s.

The normalized average evacuation effort (dvs_4) is substantially the same between the macroscopic and the microscopic setup-based models (they only differ by 3%, meaning that reaching shelters on average requires the same effort), while differences with LSM results exist, consistently with the longer average paths obtained with this model. In this case, percentage differences for dvs_4 are close to the literature acceptability threshold, while those related to absolute values ($DVS_{AVG,4}$) are under the threshold, indeed, thus remarking the general adherence between the adopted models.

4. *Discussion and final remarks*

The current work contributes to the definition of digital technologies to be applied in the context of risk assessment and mitigation strategies evaluation in HUBEs, focusing on flood risk as one of the most challenging ones. It provides a multi-step and multi-scale tool which integrates hydrodynamic and evacuation simulations in flood-prone HUBEs, to: (1) assess if and how human behavior affect risk levels; and (2) evaluate how emergency plans can be optimized, by testing the combination of number and position of gathering areas with different route choice behavior, to improve human safety.

The novelties of the work lie in the development of a multi-scale modeling framework for flood evacuation, embedded within a multi-criteria optimization process, including a validation stage against already validated models.

The following subsections further discuss the work key findings in terms of human behavior impact on the overall risk evaluation (Section 4.1), and provides insights on the tool verification with respect to well-established models, moving towards a cross comparison between simulation approaches (Section 4.2). Implications for practitioners are then pointed out in Section 4.3, while limitations and future works are addressed in Section 4.4.

4.1 Human behavior impact on the risk evaluation

Comparing Risk Indexes based on the inclusion or exclusion of human evacuation behaviors across different HUBE layouts provide valuable insights from multiple perspectives and remark the role of digital technologies that include human behavior into flood risk assessment.

From an analytical point of view, limiting flood risk assessment to hydrodynamic condition analyses can induce overestimations (or underestimations, eventually), even if RI_{EB} consider the users' motion capabilities, actually (i.e., the normalized stability index $idv_{i,j}$). Vice versa, introducing human behaviors into risk quantification (e.g., times $t_{i,j}$, lengths $d_{i,j}$, flows $f_{i,j}$, and casualties $n_{i,j}$) play a crucial role in shaping evacuation dynamics. Moreover, applications to real-world case studies could involve substantial risk variations depending on the features of the HUBEs and its population. For instance, users' distribution (together with their own physical and behavioral skills) can drastically vary based on the presence of specific intended uses, like religious buildings, hospitals, monuments, and attractions.

4.2 Comparisons between the simulation models

Comparisons between evacuation simulation models enable verification tasks. The three tested simulators on the selected case study (Square C as the riskiest HUBE) provide similar outcomes, thus highlighting the efficiency of the macroscopic model, which significantly reduces modeling effort and computational time by allowing the evaluation of multiple configurations within a single simulation while providing reliable results.

Conversely, microscopic models would necessitate the creation of different scenarios for each evacuation configuration, making the process highly time-consuming and resource intensive. In this sense, to reduce efforts on the creation of multiple cross-verification scenarios, the macroscopic model has been sued for optimization purposes, and then only the most relevant scenarios (namely, the best configuration and the "worst" scenario in terms of overall risk) were simulated using microscopic models.

In particular, considering the LSM as the main consolidated benchmark (Evans et al., 2024; Lumbroso et al., 2023; Lumbroso & Davison, 2018), differences in KPIs and RI_{IB} outcomes seem to point out satisfactory verification results. The microscopic setup-based model, instead, provides slightly different results, even though they could be traced back to the characterizing modeling logic (i.e. pedestrians generated, interacting and moving in a continuous outdoor space).

As a result, in general terms, the macroscopic model and the LSM slightly overestimate the risk for the single pedestrians by computing longer evacuation lengths and times to reach the shelters than the microscopic setup-based model. On the contrary, the microscopic setup-based model overestimates the risk for groups by computing a higher number of pedestrians unable to complete the evacuations.

Therefore, results would underline that the macroscopic model could be able to support risk assessment in HUBE affected by flood by pursuing a sustainable approach in application terms. In fact, it relies on a simple and adaptable definition of the urban network and of the localization of exposed pedestrians, while it can easily provide a comparison between different route choice strategies, also thanks to the developed KPIs and RI_{IB}. Furthermore, to the best of the authors' knowledge, the multi-objective framework adopted for the macroscopic approach is among the first in the field of pedestrian flood to integrate location and network flow models, jointly identifying optimal shelter positions and evacuation routes at a reasonable computational cost. This approach allows supporting flood risk mitigation through digital technologies to cope with emergencies and evacuation planning, and is based on reliable but expeditious analyses according to evaluations at the community-scale, like overall evacuation length, time, effort, and casualties. In particular, the latter is one of the essential targets of the proposed hierarchical method, although it seems to be still overlooked as an optimization criterion in similar studies relying on multi-objective approaches (Kazazi Darani & Bashiri, 2018). Evacuation units and districting issues from macroscopic model application could

then be tested more deeply using microscopic approaches, especially those relying on continuous pedestrian movement representation.

4.3 Practical implications

All the proposed models converge in evacuation risk assessment on the selected case studies, thus supporting reliable emergency planning from the same behavioral-based perspective. Local administrators and decision-makers can take advantage of digital tools for quick and reliable assessment through the proposed KPIs and Ris, in combination with specific analyses on evacuation facilities features within the risk mitigation process. For instance, surfaces [m^2] and/or density of evacuees [persons/m^2] at the sheltering areas can be estimated, defining their number also to avoid flow problems and physical contacts between pedestrians. To this end, uncapacitated shelters can be modified to consider limitations in maximum capacity and flow capacity restrictions along links (Saeed Osman & Ram, 2013).

Moreover, urban furniture like handrails and road signals could be also deployed to support safe areas and improve pedestrian stability and allocation along evacuation paths (Musolino et al., 2022). In this sense, districting the HUBEs into evacuation units is useful to solve logistic issues, such as planning how many emergency teams are needed for rescuers' operations (i.e., deploying evacuation units to a certain number of rescuers; considering issues related to pedestrians with reduced motion capabilities).

Beyond methodological advances, a key contribution is the framework usability in real contexts. Indeed, this approach can support decision-makers not only in evaluating evacuation efficiency under current conditions, but also in comparing alternative strategies or modified layouts of the same area.

This includes assessing the effectiveness of structural interventions such as raised platforms or structural measures to control water flow or pedestrian evacuation paths. By integrating such modifications into the simulations, the resulting impact on evacuation performance can be quantified and compared directly through risk indicators.

The risk indicators are designed to be simple to interpret, thus allowing practitioners with different backgrounds to evaluate and compare evacuation strategies, test alternative layouts of the same area, and assess their effectiveness. Through these features, the methodology extends beyond theoretical analysis and provides a practical decision-support tool directly applicable to the management of flood-prone HUBEs.

Finally, the application to an idealized case study also allows analyses based on typological features recurring in the Italian national context. For instance, the findings of this work highlight the importance of placing shelters based on a modular criterion related to the source of risk (i.e., the river), while also considering the shielding offered by building blocks to determine their optimal location. Additionally, shelter placement should aim to minimize the need for pedestrians to cross multiple crossroads, where the confluence of floodwater flows can create more severe conditions (Mignot et al., 2019). Such general outcomes could point out relevant issues in real-world HUBEs characterized by similar conditions, thus supporting the design of standard solutions, fundamental to anticipate/improve evacuation (e.g. installing road signals, wayfinding systems, and tailored urban furniture in the expected most dangerous areas).

4.4 Work limitations and future research

The scenarios used in this work can represent a consistent reference for testing and comparing simulation models and flood evacuation strategies. Nevertheless, it is worth noticing that some results could be influenced by the limited complexity of the case study, e.g. the street network does not consider factors such as variations in the streets geometry, the paving materials, or the presence of sewer systems and green areas. Such assumptions might explain the almost high concordance between the three route choice strategies (i.e., shortest, quickest, and less effortful), and the three tested modeling approaches. Indeed, differences in effects on pedestrian risk and timing emerge even considering a slightly more complex urban portion of the study case, like the square.

In future research, both the scenarios and the KPIs can be improved to consider further aspects that may respectively influence the overall urban layout and the risks for pedestrians, for instance considering the presence of budget limitations or urban constraints (e.g., cultural heritages where it would be to implement shelters). To this end, future applications should also explore real-world case studies. More complex hydrodynamic conditions could be used to investigate possible

influences on the floodwater stream, for instance including evolutionary trends over time rather than static conditions related to the event peak time.

To include a more detailed representation of real evacuation dynamics, future works should move towards the inclusion of adaptive rerouting and dynamic responses to evolving conditions (e.g. route blockage due to floodwater spreading; pedestrian density increase). Additional pedestrian features could also be introduced, to simulate weak motion capabilities for children, elderly, and people with disabilities, and different individual responses. The model should consider all these issues, being able to reroute individuals towards certain paths and shelter locations, e.g., to avoid stability threats, reduce congestion and bottlenecks and optimize exposure timings. Moreover, scenarios modelling can include dynamics in terms of timings of the disaster (e.g., day/night, weekday/holiday) and individuals' familiarity with built environment and safety procedures, boosting the applicability by decision makers especially in HUBEs affected by large variabilities in user exposure and vulnerability (e.g. touristic HUBEs).

Finally, as also remarked by previous research (Beyki et al., 2023; Huertas et al., 2020), an interesting line of investigation for computational modeling on evacuation simulation software could be the coupling of different models into a unique tool to exploit their strengths respectively. In particular, while the macroscopic model allows quick identification of the optimal configurations for the shelters positioning and to consider/compare different routing algorithms (i.e., decision-making process to select the evacuation routes), the microscopic models provide more detailed analyses considering each pedestrian interaction with the surrounding built environment, floodwater, and other pedestrians. Such kind of analysis could be fundamental for a future implementation of the graph-solving algorithm straight into a microscopic model (Quagliarini et al., 2022) with the aim of providing a unique ready-to-use simulator for flood evacuation (i.e., with no need of specific setup to be used), which would represent an increasing innovation in the field. For this purpose, traffic models relying on constrained optimal systems or tolerance-based dynamic users could be evaluated for accounting for the evacuee's selfishness while keeping the computational viability of the approach (compare, e.g., with (Bayram, 2016)).

Acknowledgments

The software license of the MassMotion simulation software was supplied to the researchers by Oaysis Ltd in the context of the Mutual Non-Disclosure Agreement "Simulating human behaviours during emergencies to improve the safety of buildings: testing and validation of the Massmotion simulation software".

REFERENCES

Arrighi, C., Pregnolato, M., Dawson, R. J. J., & Castelli, F. (2019). Preparedness against mobility disruption by floods. *Science of the Total Environment*, *654*, 1010–1022. https://doi.org/10.1016/j.scitotenv.2018.11.191

Bashir, T., Bergantino, A. S., Troiani, G., Henke, I., & Pagliara, F. (2025). Vulnerability and resilience analysis of road network: A systematic literature review using Bibliometrix. Sustainable Futures, 10. https://doi.org/10.1016/j.sftr.2025.101142

Bayram, V. (2016). Optimization models for large scale network evacuation planning and management: A literature review. *Surveys in Operations Research and Management Science*, *21*(2), 63–84. https://doi.org/10.1016/j.sorms.2016.11.001

Bayram, V., & Yaman, H. (2018). Shelter Location and Evacuation Route Assignment Under Uncertainty: A Benders Decomposition Approach. *Transportation Science*, *52*(2), 416–436. https://doi.org/10.1287/trsc.2017.0762

Bernardini, G., Romano, G., Soldini, L., & Quagliarini, E. (2021). How urban layout and pedestrian evacuation behaviours can influence flood risk assessment in riverine historic built environments. *Sustainable Cities and Society*, *70*. https://doi.org/10.1016/j.scs.2021.102876

Beyki, S. M., Santiago, A., Laím, L., & Craveiro, H. D. (2023). Evacuation Simulation under Threat of Wildfire—An Overview of Research, Development, and Knowledge Gaps. *Applied Sciences*, *13*(17), 9587. https://doi.org/10.3390/app13179587

Bianchi, C., & Salvati, P. (2024). *Rapporto Periodico sul Rischio posto alla Popolazione italiana da Frane e inondazioni - Anno 2023*. https://doi.org/10.30437/report2023

Bloomberg, M., & Burden, A. (2006). *New York City Pedestrian Level of Service Study*. New York, USA.

Borrmann, A., Kneidl, A., Köster, G., Ruzika, S., & Thiemann, M. (2012). Bidirectional coupling of macroscopic and microscopic pedestrian evacuation models. *Safety Science*, *50*(8), 1695–1703. https://doi.org/10.1016/j.ssci.2011.12.021

Carrozzino, M., Piacentini, V., Tecchia, F., & Bergamasco, M. (2012). Interactive visualization of crowds for the rescue of cultural heritage in emergency situations. *SCIRES-IT - SCIentific RESearch and Information Technology*, *2*(1), 133–148. https://doi.org/10.2423/i22394303v2n1p133

Chraibi, M., Tordeux, A., Schadschneider, A., & Seyfried, A. (2018). *Modelling of Pedestrian and Evacuation Dynamics BT - Encyclopedia of Complexity and Systems Science* (R. A. Meyers, Ed.). Berlin, Heidelberg. https://doi.org/10.1007/978-3-642-27737-5_705-1

Coutinho-Rodrigues, J., Tralhão, L., & Alçada-Almeida, L. (2012). Solving a location-routing problem with a multiobjective approach: the design of urban evacuation plans. *Journal of Transport Geography*, *22*, 206–218. https://doi.org/10.1016/j.jtrangeo.2012.01.006

Cox, R. J., Shand, T. D., & Blacka, M. J. (2010). Australian Rainfall & Runoff revision project 10: Appropriate safety criteria for people. In *Engineers Australia*. https://doi.org/10.1038/103447b0

Dempe, S., Kalashnikov, V., Pérez-Valdés, G. A., & Kalashnykova, N. (2015). *Bilevel Programming Problems*. Berlin, Heidelberg. https://doi.org/10.1007/978-3-662-45827-3

De Padova, D., Mossa, M., Chiaia, G., Chimienti, G., Mastrototaro, F., & Adamo, M. (2024). Optimized environmental monitoring: innovative solutions to combat climate change. *SCIRES-IT - SCIentific RESearch and Information Technology*, *14*(Special Issue), 43–52. https://doi.org/10.2423/i22394303v14Sp43

Dias, C., Rahman, N. A., & Zaiter, A. (2021). Evacuation under flooded conditions: Experimental investigation of the influence of water depth on walking behaviors. *International Journal of Disaster Risk Reduction*, *58*, 102192. https://doi.org/10.1016/j.ijdrr.2021.102192

Evans, B., Lam, A., West, C., Ahmadian, R., Djordjević, S., Chen, A., & Pregnolato, M. (2024). A combined stability function to quantify flood risks to pedestrians and vehicle occupants. *Science of The Total Environment*, *908*, 168237. https://doi.org/10.1016/j.scitotenv.2023.168237

Ferreira, T. M., & Santos, P. P. (2020). An Integrated Approach for Assessing Flood Risk in Historic City Centres. *Water*, *12*(6), 1648. https://doi.org/10.3390/w12061648

Guo, P., Xia, J., Zhou, M., Falconer, R. A. ., Chen, Q., & Zhang, X. (2018). Selection of optimal escape routes in a flood-prone area based on 2D hydrodynamic modelling. *Journal of Hydroinformatics*, *20*(6), 1310–1322. https://doi.org/10.2166/hydro.2018.161

Hamacher, H. W. W., & Tjandra, S. A. A. (2002). Mathematical modelling of evacuation problems: state of the art. In M. Schreckenberg & S. D. Sharma (Eds.), *Pedestrian and Evacuation Dynamics 2002* (Vol. 24, pp. 227–266). Springer Verlag. https://doi.org/citeulike-article-id:6650160

Helbing, D., & Molnár, P. (1995). Social Force Model for Pedestrian Dynamics. *Physical Review E*, *51*(5), 4282–4286. https://doi.org/10.1103/PHYSREVE.51.4282

HR Wallingford Ltd. (2021). *Life Safety Model (LSM). LSM version 3.2 Technical reference guide - MCT0243.*

Hsiao, C.-C., Sun, M.-C., Chen, A. Y., & Hsu, Y.-T. (2021). Location problems for shelter-in-place deployment: A case study of vertical evacuation upon dam-break floods. *International Journal of Disaster Risk Reduction*, *57*. https://doi.org/10.1016/j.ijdrr.2021.102048

Huertas, J. A., Duque, D., Segura-Durán, E., Akhavan-Tabatabaei, R., & Medaglia, A. L. (2020). Evacuation dynamics: a modeling and visualization framework. *OR Spectrum*, *42*(3), 661–691. https://doi.org/10.1007/s00291-019-00548-x

Jiang, Y., Chen, B., Li, X., & Ding, Z. (2020). Dynamic navigation field in the social force model for pedestrian evacuation. *Applied Mathematical Modelling*, *80*, 815–826. https://doi.org/10.1016/j.apm.2019.10.016

Kazazi Darani, S., & Bashiri, M. (2018). A multi-district asset protection problem with time windows for disaster management. *International Journal of Engineering, Transactions B: Applications*, *31*(11), 1929–1934. https://doi.org/10.5829/ije.2018.31.11b.17

Lee, Y.-H., Keum, H.-J., Han, K.-Y., & Hong, W.-H. (2021). A hierarchical flood shelter location model for walking evacuation planning. *Environmental Hazards*, *20*(4), 432–455. https://doi.org/10.1080/17477891.2020.1840327

Li, Y., Hu, B., Zhang, D., Gong, J., Song, Y., & Sun, J. (2019). Flood evacuation simulations using cellular automata and multiagent systems -a human-environment relationship perspective. *Int. Journal of Geographical Inf. Science*, *33*(11), 2241–2258. https://doi.org/10.1080/13658816.2019.1622015

Liu, X., & Lim, S. (2018). An agent-based evacuation model for the 2011 Brisbane City-scale riverine flood. *Natural Hazards*, *94*(1), 53–70. https://doi.org/10.1007/s11069-018-3373-1

Lopes, A. C. R., Rezende, O. M., & Miguez, M. G. (2025). Urban resilience to floods in the context of the disaster risk management cycle: a literature review. *Journal of Hydrology*, 662. https://doi.org/10.1016/j.jhydrol.2025.133827

Lumbroso, D., & Davison, M. (2018). Use of an agent-based model and Monte Carlo analysis to estimate the effectiveness of emergency management interventions to reduce loss of life during extreme floods. *Journal of Flood Risk Management*, *11*, S419–S433. https://doi.org/10.1111/jfr3.12230

Lumbroso, D., Davison, M., & Wetton, M. (2023). Development of an agent-based model to improve emergency planning for floods and dam failures. *Journal of Hydroinformatics*, *25*(5), 1610–1628. https://doi.org/10.2166/hydro.2023.194

Ma, Y., Xu, W., Qin, L., & Zhao, X. (2019). Site Selection Models in Natural Disaster Shelters: A Review. *Sustainability*, *11*(2), 399. https://doi.org/10.3390/su11020399

Marinelli, F., Pizzuti, A., Romano, G., Bernardini, G., & Quagliarini, E. (2025). *An ILP formulation to optimize flood evacuation paths by minimizing pedestrian speed, length and effort*. Retrieved September 24, 2025, from http://arxiv.org/abs/2504.12958

Mignot, E., Li, X., & Dewals, B. (2019). Experimental modelling of urban flooding: A review. *Journal of Hydrology*, *568*, 334–342. https://doi.org/10.1016/j.jhydrol.2018.11.001

Musolino, G., Ahmadian, R., & Xia, J. (2022). Enhancing pedestrian evacuation routes during flood events. *Natural Hazards*. https://doi.org/10.1007/s11069-022-05251-9

Quagliarini, E., Bernardini, G., Romano, G., & D'Orazio, M. (2022). Simplified flood evacuation simulation in outdoor built environments. Preliminary comparison between setup-based generic software and custom simulator. *Sustainable Cities and Society*, *81*, 103848. https://doi.org/10.1016/J.SCS.2022.103848

Ronchi, E. (2020). Developing and validating evacuation models for fire safety engineering. *Fire Safety Journal*, 103020. https://doi.org/10.1016/j.firesaf.2020.103020

Saaty, T. L. (1980). *The analytic hierarchy process*, MacGraw-Hill, New York International Book Company.

Saeed Osman, M., & Ram, B. (2013). Two-phase evacuation route planning approach using combined path networks for buildings and roads. *Computers & Industrial Engineering*, *65*(2), 233–245. https://doi.org/10.1016/j.cie.2013.03.001

Spearpoint, M., Arnott, M., Xie, H., Gwynne, S., & Templeton, A. (2024). Comparative analysis of two evacuation simulation tools when applied to high-rise residential buildings. *Safety Science*, *175*, 106515. https://doi.org/10.1016/j.ssci.2024.106515

UNDRR. (2024). Sendai Framework Terminology. Retrieved February 22, 2024, from https://www.undrr.org/drr-glossary/terminology

Zhu, Y., Li, H., Wang, Z., Li, Q., Dou, Z., Xie, W., Zhang, Z., Wang, R., Nie, W. (2022). Optimal Evacuation Route Planning of Urban Personnel at Different Risk Levels of Flood Disasters Based on the Improved 3D Dijkstra's Algorithm. *Sustainability (Switzerland)*, *14*(16), 10250. https://doi.org/10.3390/su141610250

Zhu, Z., Zhou, L., Zhang, C., Lin, B., Cui, Y., & Che, M. (2018). Modeling of Macroscopic Building Evacuation Using IFC Data. *ISPRS Int. Journal of Geo-Information*, *7*(8), 302. https://doi.org/10.3390/ijgi7080302

Zhuo, L., & Han, D. (2020). Agent-based modelling and flood risk management: A compendious literature review. *Journal of Hydrology*, *591*, 125600. https://doi.org/10.1016/j.jhydrol.2020.125600